SCIENCE CHINA
Information Sciences

• RESEARCH PAPER •

June 2018, Vol. 61 060414:1–060414:9
https://doi.org/10.1007/s11432-018-9396-7

Special Focus on Flexible Electronics Technology

Flexible ultra-wideband rectangle monopole antenna with O-slot insertion design

Sihong CHEN, Taisong PAN*, Zhuocheng YAN, Min GAO & Yuan LIN*

State Key Laboratory of Electronic Thin Films and Integrated Devices, University of Electronic Science and Technology of China, Chengdu 610054*, China*

Received 4 January 2018/Revised 15 March 2018/Accepted 21 March 2018/Published online 11 May 2018

Abstract Slot insertion design has proven to be an effective method to increase the bandwidth in the design of microstrip antenna. In this paper, the slot insertion design is applied to the flexible ultra-wideband (UWB) antenna. A flexible rectangular UWB monopole antenna is proposed and fabricated with O-slot design using the transfer printing method. By simulating the influence of O-slot design parameters on electromagnetic performance of the antenna, an optimized antenna design is obtained to keep the reflection coefficient under −10 dB with the frequencies ranging from 3.5 to 17.8 GHz when the antenna is bent with curvature radius as small as 11 mm. The effect of bending on the reflection coefficient is analyzed. Mechanical simulations indicate that the existence of O-slot can reduce the strain concentration on the metal layer of antenna, which enhances the flexibility of the antenna.

Keywords slot insertion, rectangular monopole antenna, ultra-wideband, flexibility, transfer printing

Citation Chen S H, Pan T S, Yan Z C, et al. Flexible ultra-wideband rectangle monopole antenna with O-slot insertion design. Sci China Inf Sci, 2018, 61(6): 060414, https://doi.org/10.1007/s11432-018-9396-7

1 Introduction

Flexible electronics, with the ability to stretch, twist and bend, have showed many exciting applications in wearable electronics, artificial skins and other areas [1–5]. For an integrated flexible electronic system, wireless communication capability is becoming a necessary element. Therefore, designing an antenna which can tolerate the deformation plays a key role in the design of flexible integrated electronic system. Ultra-wideband (UWB) wireless communication, due to its high data transmission rate, low power dissipation and resistance to interfere, becomes a promising candidate for novel wireless network [6–8]. As the core of UWB applications, the design of UWB antenna has been intensively studied in recent years. Among the numerous kinds of UWB antennas proposed, planar monopole antenna is considered as a suitable design to meet the requirement of easy-fabrication, integration and miniaturization [9]. Especially when a slot is inserted into the radiator of antenna, miniaturization of the planar monopole antenna can be achieved and the performance of the antenna can be even enhanced [10–15]. Several studies have been reported that inserting U-slot or Q-slot into the radiator of UWB planar monopole antenna can effectively improve the impedance matching and increase the bandwidth [11, 12, 14]. However, there are still some concerns in current studies to confine the further application of these UWB antenna in the flexible electronics. First, the slot-inserted UWB antennas studied currently are fabricated on the hard and planar substrates, which lack the deformation ability required for flexible electronics. Second, the

* Corresponding author (email: tspan@uestc.edu.cn, linyuan@uestc.edu.cn)

deformation may induce the change of structural parameters of the antenna resulting in the deterioration of its characteristics, especially when a slot exists in the antenna. Therefore, it is necessary to explore an antenna which is based on flexible substrate and keeps electromagnetic and mechanic properties stable with large deformation. Another important issue in the design and fabrication of flexible slot-inserted UWB antenna is choosing a stretchable substrate and developing corresponding fabrication techniques. Polyimide (PI) is the most common substrate material used in current flexible antenna design [16]. PI can withstand the high temperature during the deposition of metal on the substrate, which makes it possible to use conventional lift-off method to directly prepare the metal pattern of the antenna on the PI substrate. However, the elastic modulus of PI is about 2.5 GPa, which is much larger than many other soft silicone materials (e.g., polydimethylsiloxane (PDMS): ∼1 MPa, Ecoflex: ∼60 kPa). The large elastic modulus of PI leads to limited flexibility of substrate. The PI substrate is only bendable but not stretchable. The lack of stretchability of PI substrate makes it difficult to realize conformal contact to non-developable surfaces, like human skin on the joint. Thus, it is necessary to apply a substrate with much smaller elastic modulus in the design of flexible antenna. PDMS is a kind of silicone materials with the elastic modulus about 1 MPa, which is more than 1000 times smaller than PI. Moreover, compared with the previous reported flexible dielectric materials used in antennas designs, such as textile and fabric, PDMS has significantly higher dielectric constant [17–28], which makes it suitable for applications in the design of compact flexible antennas. Although the PDMS has appropriate mechanical and dielectric properties, it cannot withstand the increased temperature when directly depositing metal layer using a physical vapor deposition method, which is essential in the lift-off method. With the low temperature tolerance of PDMS, alternative preparation method is required for the metal layer of antenna on PDMS substrate.

In this paper, a flexible UWB rectangular monopole antenna (RMA) inserted with an O-slot is designed and fabricated. The insertion strategy of O-slot and its effect on the impedance bandwidth of the antenna are discussed with simulation results. By using the transfer printing process, an antenna with optimized design is fabricated on PDMS substrate. The flexibility of the antenna is demonstrated by the study on the mechanical and electromagnetic properties of the antenna bended on surfaces with different curvature radius, which is supported by the simulation and experimental results.

2 Methods

2.1 Finite element analysis

The finite element analysis of strain distribution was completed with the commercial software ABAQUS. The model of the hexahedron element (C3D8R) was used in the PDMS substrate, while the composite shell element (S4R) model was adopted in the copper foil of radiator. The mechanical behavior of copper was described by an ideal elastic-plastic constitutive relation and the criterion that elastic stretchability corresponds to section in which the Mises stresses in the metal layer are beyond the yield strain (∼357 MPa for Cu and ∼0.3% yield strain) across half the width of one section was used. As for the elastomeric PDMS substrate, a typical hyper-elastic constitutive relation, the MooneyRivlin law, was adopted to describe the mechanic properties (elastic modulus $E_{\mathrm{PDMS}} = 1$ MPa and Poissons ratio $\nu_{\mathrm{PDMS}} = 0.49$). The meshes were refined to ensure computational accuracy.

2.2 Antenna fabrication

The PDMS substrate was prepared by mixing the Sylgard 184 monomer with the curing agent in a volume ratio of 10:1 and then degassed under primary vacuum for 30 min to remove trapped air bubbles. After that, the polymerization of PDMS was cured at 85°C for an hour. The copper radiator was defined by using the commercial cutting machine (Silhouette Cameo, USA). The copper foil (the purity is 99.98% and the conductivity is $\sigma = 5.7$–5.8×10^7 S/m) with the thickness of 0.1 mm attached on the water-soluble cellulose tape (Aquasol Corporation, USA) was carved into the designed pattern. After carving,

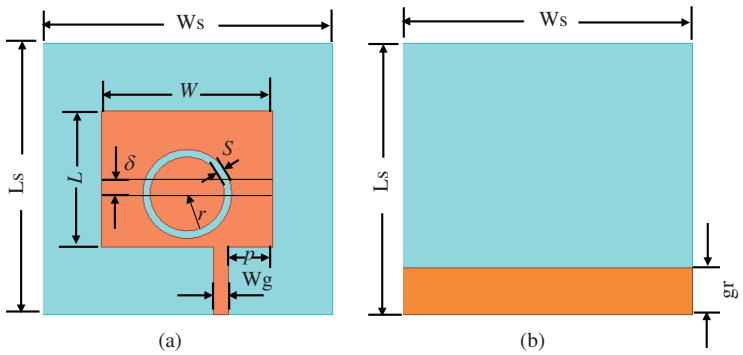

Figure 1 (Color online) (a) Top view and (b) bottom view of the geometric layout of the O-slot UWB antenna.

the patterned copper foil was delaminated from the cutting mat, followed by transfer printing the foil onto the flexible PDMS substrate and then put the device into the pure water for several minutes to dissolve the tape.

2.3 Simulation and measurement

For the reflection coefficient simulation of the antenna, the HFSS finite element solver was employed. In the simulation domain, the driven model of solution type was used. The model of PDMS was created with the permittivity of 2.68 and loss tangent of 0.04, while the copper foil was assigned with finite conductivity boundary with the conductivity of $\sigma = 5.8 \times 10^7$ S/m and an air-box assigned with radiation boundary was created around the antenna with adding space of a quarter of wavelength at 3.5 GHz. The reflection coefficient was tested by Agilent Technologies E8363C vector network analyzer (10 MHz–40 GHz).

3 Results and discussion

3.1 Structure designation

Inspired by U-Slot Monopole antennas which successfully improve the impedance matching to achieve UWB applications by inserting a slot [11,12], we have designed a kind of antenna with an O-slot inserted on the rectangle radiator in order to improve performance and achieve miniaturization. Compared with the reported U-slot or Q-slot antenna, O-slot has simpler design and achieves better impedance matching to obtain broader bandwidth, which makes it have greater advantages in UWB applications. Figure 1 illustrates the geometry of the proposed antenna. Polydimethylsiloxane (PDMS) with a thickness of 1.6 mm and a dimension of Ls × Ws = 36.6 mm × 39 mm is used for the antennas dielectric layer. An $L \times W$ = 18.3 mm × 23 mm rectangle radiator is placed on top of the substrate. A rectangle ground metal strip is attached on the backside of the substrate with the dimension of Ls × gr = 36.6 mm × 6.3 mm. Other dimensions are summarized in Table 1. The coaxial transmission line with the characteristic impedance of 50 Ω is used to feed the antenna. For a UWB antenna, one of main purposes to insert a slot is adjusting the impedance matching over the frequency bandwidth. However, the existence of the inserted slot may also affect the current distribution on the radiator of antenna, which may have negative influence on the performance of the antenna. Therefore, the current distributions on the radiator of the antenna inserted with an O-slot are simulated to confirm the feasibility of this design. As demonstrated in Figure 2, the current distributions of RMAs with and without an O-slot are simulated at frequencies of 4.0, 9.6 and 16.8 GHz, respectively. It can be seen from Figure 2(a)–(c) that the surface current density on the middle of the rectangle patch is relatively weak, which means the O-slot with suitable size can be inserted in this region to change the impedance matching with little influence on the current distribution. The simulation results of the surface current distribution on the radiator of RMA with an inserted O-slot confirm this prediction. As shown in Figure 2(d)–(f), the surface current density of the O-slot inserted antenna is similar with the one of the antenna without slot. Meanwhile, as indicated by the simulated

Table 1 Parameters of the antenna shown in Figure 1

Parameter	Description	Value (mm)
Ls	Substrate length	36.6
Ws	Substrate width	39
L	Radiator length	18.3
W	Radiator width	23
S	Slot width	1
δ	Deviation distance of O-slot	2
p	Feeding position	6
Wg	Microstrip width	2
r	Radius of O-slot	6
h	Thickness of dielectric layer	1.6
gr	Ground length	6.3

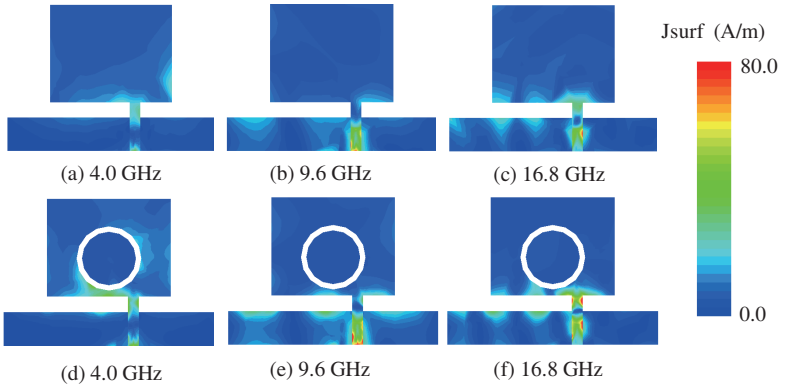

Figure 2 (Color online) Simulation results of surface current distributions on the radiator of UWB RMA at three representative frequencies. (a)–(c) UWB RMA without O-slot; (d)–(f) UWB RMA with O-slot.

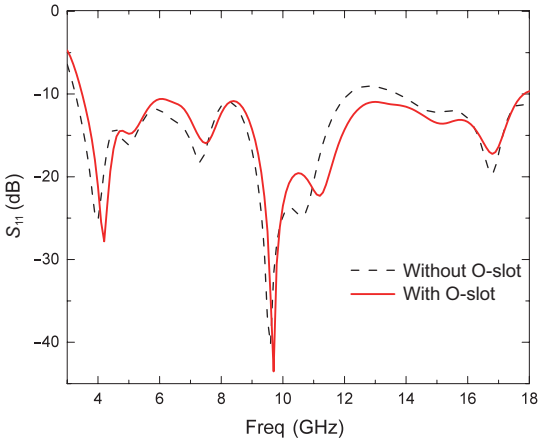

Figure 3 (Color online) Simulated frequency response of the UWB RMA with/without O-slot.

relation between the reflection coefficient (S_{11}) and the frequency of RMA with/without an O-slot in Figure 3, the impedance bandwidth of RMA is improved by the insertion of an O-slot. In the frequencies ranging from 12.2 to 13.7 GHz, the S_{11} parameter of RMA without an O-slot is above −10 dB, which indicates poor impedance matching of RMA without an O-slot in this frequency region. When the O-slot is inserted, the S_{11} parameter of RMA at frequency range from 12.2 to 13.7 GHz is improved to be below −10 dB, making the RMA have larger impedance bandwidth ranging from 3.5 to 17.8 GHz and suitable for the UWB applications.

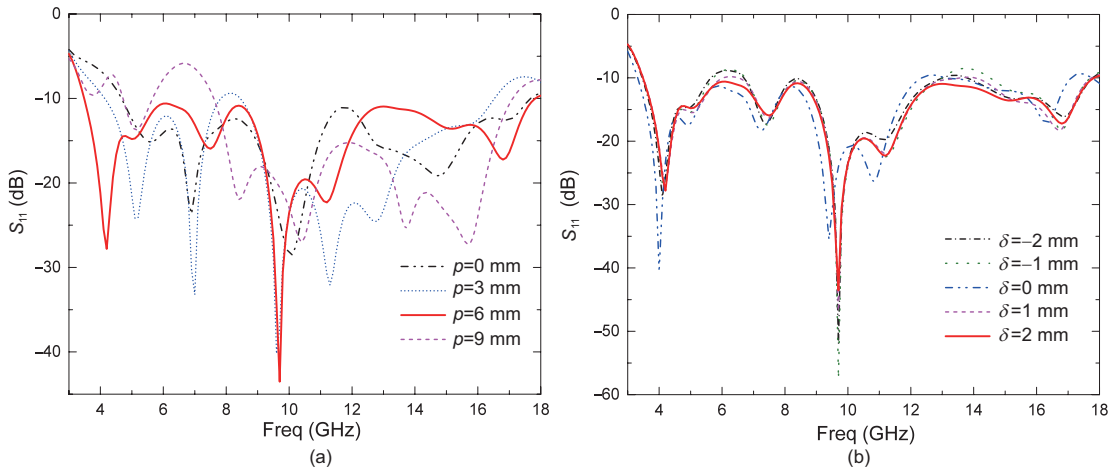

Figure 4 (Color online) The simulated reflection coefficient of O-slot inserted UWB RMA with different (a) feed position, p, and (b) deviation distance of the O-slot, δ. The other parameters of antenna are fixed with the parameters shown in Table 1.

3.2 Electromagnetic performance optimization

Although the insertion of an O-slot has been confirmed to be an effective method to improve the S_{11} parameter of a UWB RMA on a PDMS substrate, the influence of insertion parameters, including feeding position (p), deviation distance of the O-slot (δ), slot width (s) and slot radius (r), is worth more detailed discussion for further improvement of the electromagnetic performance of the UWB RMA with an inserted O-slot. In all of the following paremetric studies, only one parameter varies during each optimization, while the others are fixed to those of Table 1.

Figure 4 shows the simulated reflection coeffcient versus the feeding position and the deviation distance of the O-slot respectively. Significant impact on the antennas performance is observed with the change of the feeding position (p). By varying the feeding position, not only the bandwidth will be changed, but also the strength of the reflection coefficient and the location of the resonant frequency will be affected due to the changes of local current distributions. It can be seen that with the feeding position moving to the center of the rectangle, the bandwidth first increases and then decreases, and the band-rejection appears at the frequency ranging from 6 to 8 GHz when p is set to 9 mm. Through the parametric analysis, the maximum bandwidth ranging from 3.5 to 17.8 GHz is obtained at $p = 6$ mm and another slightly large bandwidth is achieved at $p = 0$ mm (see Figure 4(a)). The effects of the deviation distance of the O-slot (δ) are analysed and shown in Figure 4(b). As few of the currents of this antenna are confined in the middle, there is little influence on the antennas performance when varies from -2 to 2 mm. At the same time, it can be noted that the band rejection at the frequency ranging from 12.1 to 13.7 GHz appears when the slot is inserted in the middle. The improved reflection coefficient of the antenna can be attributed to the better matching between the characteristic impedance and the coaxial transmission line, which is caused by the deviation of the position of O-slot from the center. Finally, $\delta =$ 2 mm is adopted, where the largest bandwidth ranging from 3.5 to 17.8 GHz is realized.

As indicated by Figure 5, the performance of the UWB RMA, such as impedance matching, can be further optimized by adjustment of the dimensional parameters of the O-slot. By adjusting the width of the slot (s), the S-parameter in the high frequency range will be affected, especially in the range from 12 to 18 GHz. In this frequency range, the strength of reflection coefficient at the last resonant frequency gradually increases with a larger s value. However, when s increases, a band rejection appears at the frequencies between 12 and 14 GHz. When s is set to 1 mm, S_{11} satisfies the requirement (below -10 dB) and an appropriate strength of reflection coefficient at the last resonant frequency can be obtained. It is also observed that the strength of the resonance becomes larger with increase of r. But the band-rejection appears when r is greater or less than 6 mm, which makes 6 mm be the optimized r value. The simulation results show that the resonance frequency is stable with different s and r values. The stability of the

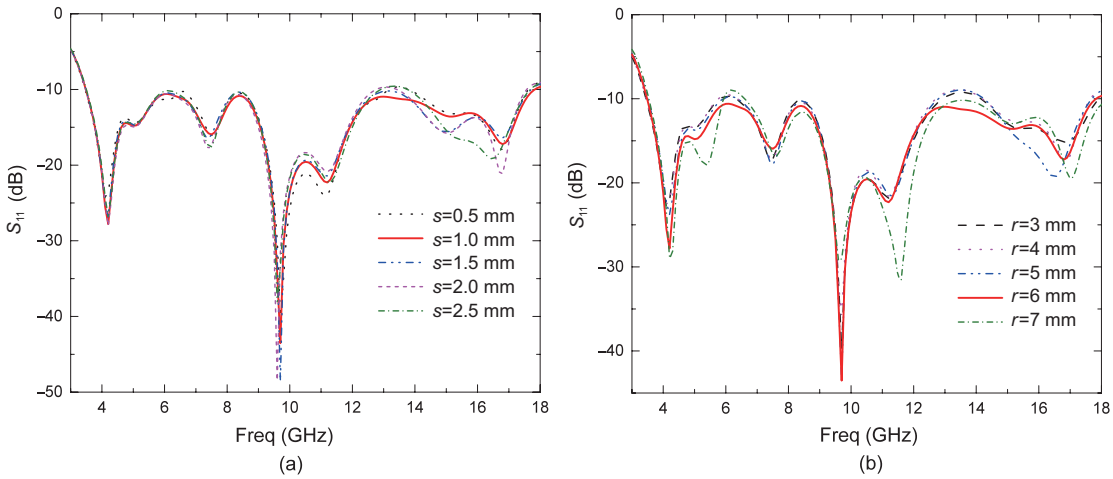

Figure 5 (Color online) The simulated reflection coefficient of O-slot inserted UWB RMA with (a) different width of O-slot, s, and (b) different radius of O-slot, r. The other parameters of antenna are fixed with the parameters shown in Table 1.

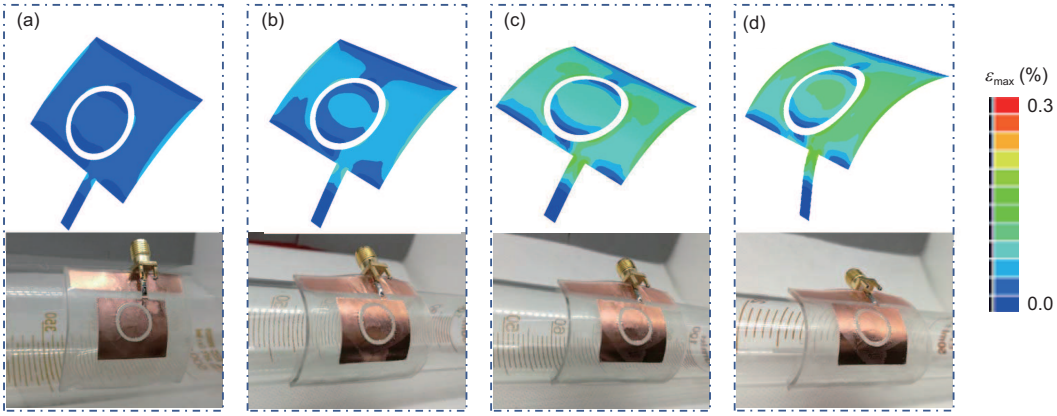

Figure 6 (Color online) FEA results of the strain distribution on Cu layer and the corresponding optical images of the antenna with O-slot when attached on cylinders with different curvature radius. (a) $R_{\rm bend}$ = 28 mm; (b) $R_{\rm bend}$ = 20 mm; (c) $R_{\rm bend}$ = 13 mm; (d) $R_{\rm bend}$ = 11 mm.

resonance frequency can be attributed to the current distribution on the radiator of antenna. It can be seen from Figure 2 that the current on radiator is mainly concentrated along the margin of rectangle radiator, so the change of slot radius results in little influence on the current distribution of the antenna. However, the change of the radius of the slot will affect the antennas impedance, which results in the change of the strength of the resonance. Lastly, s = 1 mm and r = 6 mm are fixed in the final design, in which radiation performance satisfies the demands and the reflection coefficient (S_{11}) maintains under −10 dB at the frequency ranging from 3.5 to 17.8 GHz.

3.3 Mechanical analysis and experimental characterization

With the optimized design parameters, the UWB RMA is experimentally fabricated. Since the PDMS substrate cannot withstand high temperature, the radiator of the antenna is prepared with copper foil first and then transferred to the PDMS substrate by a transfer printing method (see Section 2). For the flexible UWB RMA, its mechanical performance plays a key role in determining the reliability of the antenna during the deformation in applications. The strain distributions on the Cu layer of the O-slot inserted RMA with PDMS substrate are derived from the finite element analysis (FEA) results with bending radii of 11, 13, 20 and 28 mm, as presented in the upper panel of Figure 6. Although the strain on the Cu layer increases with a smaller bending radius, the strain on the Cu layer keeps lower than

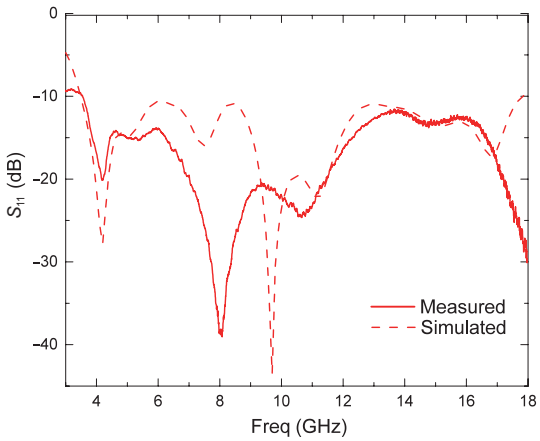

Figure 7 (Color online) Simulated (dashed) and measured (solid) S_{11} parameters of the UWB RMA with O-slot at the frequencies ranging from 3 to 18 GHz

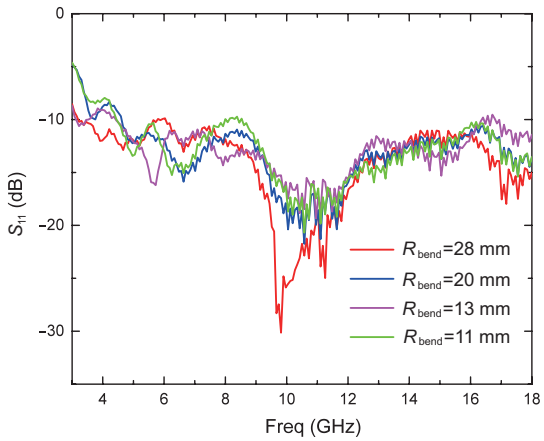

Figure 8 (Color online) Measured reflection coefficient of the UWB RMA with O-slot when attached on cylinders of different curvature radius.

0.3% when the bending radius is as small as 11 mm, which suggests that the elastic-plastic transition of Cu will not happen within the bending radius of 11 mm [29–32]. Moreover, no obvious deformation of the slot structure can be observed in the FEA results when the RMA is bent. As the electromagnetic performance of the slot-inserted RMA is strongly dependent on the structure of the slot, the stability of slot structure prevents any possible sharp change of the electromagnetic performance of the RMA, such as the reflection coefficient. The corresponding optical images are also demonstrated in the lower panel of Figure 6, which indicate that the RMA with a PDMS substrate can be attached on the curved surface without additional fixture and paste. The conformal contact between the curved surface and the RMA can be attributed to the low modulus of the PDMS substrate. With the elastic modulus of the substrate around 1 MPa, the bending stiffness of the RMA with the PDMS substrate is significantly smaller than the antenna fabricated with PI substrate, which allows the former to be easily attached on a curved surface.

The reflection coefficient of the as-fabricated UWB RMA with a PDMS substrate is measured to experimentally evaluate the electromagnetic performance of the antenna. Figure 7 shows the measured S_{11} parameter and the corresponding simulation result of the antenna without bending at the frequency ranging from 3 to 18 GHz. The measured result is in good agreement with the simulated one, which indicates the S_{11} parameter of the as-fabricated antenna maintains under -10 dB within the frequency ranging from 3.5 to 17.8 GHz and satisfies the radiation performance required for a UWB antenna. However, there is an obvious difference between measured result and simulated one when the frequency is above 15 GHz. This may be caused by deformation of the radiator occurred during the process of the transfer printing, which resulted in the impedance mismatch. The S_{11} parameters measured at frequencies ranging from 3 to 18 GHz, with bending radii of 11, 13, 20 and 28 mm, are shown in Figure 8. Although the reflection of the UWB RMA increases with the decreasing bending radius, the S_{11} parameter of the antenna keeps lower than -10 dB at the frequencies ranging from 6 to 16.5 GHz for all these bending radius values. It can also be noted that the relation between the frequency and the S_{11} parameter significantly changes when the bending radius reduces from 28 to 20 mm. But when the bending radius is below 20 mm, the change of the frequency dependence of S_{11} parameter is much less obvious. The different sensitivity with the bending radius may be caused by the non-linear relation between the bending radius and effective antenna length. For the UWB RMA, the reflection of antenna highly depends on the effective antenna length. However, the antenna length is determined not only by the physical length of the antenna, but also by the effective electric length. The change of the bending radius from 28 to 11 mm leads to the decrease of maximum radiation field, which caused the significant reduction of the effective antenna length resulting in the obvious change of the antennas performance, especially, in the range of 10 to 12 GHz. When the bending radius is small enough, the effective antenna length is not

sensitive to the change of structure parameters induced by bending, which leads to few obvious changes in the frequency dependence of S_{11} parameter.

4 Conclusion

In this paper, a flexible UWB rectangular monopole antenna with an O-slot was designed and fabricated on a PDMS substrate to realize ultra-wideband impedance bandwidth and conformal contact with a curved surface. The insertion strategies of the O-slot, including the structure design and the electromagnetic performance optimization, are discussed with simulation results. The simulation results indicate that the feeding position of the O-slot has great influence on the antennas characteristics. After successful fabrication of the antenna with the transfer printing method, the relation between the S_{11} parameter and the frequency were measured with bending radii of 0, 11, 13, 20 and 28 mm. The measured result with no bending (bending radius of 0 mm) is found to be in good agreement with the simulation predictions, which further confirms the validity of the simulation results. Although the reflection of antenna increases with the decreasing bending radius, the S_{11} parameter of the antenna keeps below -10 dB at the frequency ranging from 6 to 16.5 GHz, which indicates the antenna is capable of being used as UWB antenna even with bending radius as small as 11 mm. By this study, a compact, flexible, and ultra-broad antenna is demonstrated and expected to be a potential candidate in the field of flexible antenna for wearable and implantable radio frequency devices.

Acknowledgements This work was supported by National Basic Research Program of China (973) (Grant No. 2015CB351905), Technology Innovative Research Team of Sichuan Province of China (Grant No. 2015TD0005), and 111 project (Grant No. B13042).

References

1 Lacour S P, Courtine G, Guck J. Materials and technologies for soft implantable neuroprostheses. Nat Rev Mater, 2016, 1: 16063
2 Kim D H, Lu N, Ma R, et al. Epidermal electronics. Science, 2011, 333: 838–843
3 Son D, Lee J, Qiao S, et al. Multifunctional wearable devices for diagnosis and therapy of movement disorders. Nat Nanotech, 2014, 9: 397–404
4 Jeong J W, Yeo W H, Akhtar A, et al. Materials and optimized designs for human-machine interfaces via epidermal electronics. Adv Mater, 2013, 25: 6839–6846
5 Yeo W H, Kim Y S, Lee J, et al. Multifunctional epidermal electronics printed directly onto the skin. Adv Mater, 2013, 25: 2773–2778
6 Miller L E. Why UWB? A Review of Ultrawideband Technology. Gaithersburg: National Institute of Standards and Technology, 2003. 1–72
7 Liang J X, Chiau C C, Chen X D, et al. Study of a printed circular disc monopole antenna for UWB systems. IEEE Trans Antenn Propagat, 2005, 53: 3500–3504
8 Choi S H, Park J K, Kim S K, et al. A new ultra-wideband antenna for UWB applications. Microw Opt Technol Lett, 2004, 40: 399–401
9 Vendik I B, Rusakov A, Kanjanasit K, et al. Ultrawideband (UWB) planar antenna with single-, dual-, and triple-band notched characteristic based on electric ring resonator. Antenn Wirel Propag Lett, 2017, 16: 1597–1600
10 Bhalla R, Shafai L. Broadband patch antenna with a circular arc shaped slot. In: Proceedings of IEEE Antennas and Propagation Society International Symposium, San Antonio, 2002. 394–397
11 Deshmukh A, Ray K. Analysis of broadband variations of U-slot cut rectangular microstrip antennas. IEEE Antenn Propag Mag, 2015, 57: 181–193
12 Lee K F, Yang S L S, Kishk A A, et al. The versatile U-slot patch antenna. IEEE Antenn Propag Mag, 2010, 52: 71–88
13 Lee K F, Yang S L S, Kishk A A. Dual- and multiband U-slot patch antennas. Antenn Wirel Propag Lett, 2008, 7: 645–647
14 Weigand S, Huff G H, Pan K H, et al. Analysis and design of broad-band single-layer rectangular u-slot microstrip patch antennas. IEEE Trans Antenn Propagat, 2003, 51: 457–468
15 Yeboah-Akowuah B, Kallos E, Palikaras G, et al. A novel compact planar inverted-F antenna for biomedical applications in the MICS band. In: Proceedings of IEEE European Conference on Antennas and Propagation, The Hague, 2014. 822–824
16 Khaleel H R, Al-Rizzo H M, Rucker D G, et al. A compact polyimide-based UWB antenna for flexible electronics. Antenn Wirel Propag Lett, 2012, 11: 564–567

17 Agneessens S, Rogier H. Compact half diamond dual-band textile HMSIW on-body antenna. IEEE Trans Antenn Propagat, 2014, 62: 2374–2381
18 Agneessens S, Lemey S, Vervust T, et al. Wearable, small, and robust: the circular quarter-mode textile antenna. Antenn Wirel Propag Lett, 2015, 14: 1482–1485
19 Yan S, Soh P J, Vandenbosch G A E. Dual-band textile MIMO antenna based on substrate-integrated waveguide (SIW) technology. IEEE Trans Antenn Propagat, 2015, 63: 4640–4647
20 Soh P J, Vandenbosch G A E, Ooi S L, et al. Design of a Broadband All-Textile Slotted PIFA. IEEE Trans Antenn Propagat, 2012, 60: 379–384
21 El Hajj W, Person C, Wiart J. A novel investigation of a broadband integrated inverted-F antenna design; application for wearable antenna. IEEE Trans Antenn Propagat, 2014, 62: 3843–3846
22 Wang Z, Lee L Z, Psychoudakis D, et al. Embroidered multiband body-worn antenna for GSM/PCS/WLAN communications. IEEE Trans Antenn Propagat, 2014, 62: 3321–3329
23 Zhu S, Langley R. Dual-band wearable textile antenna on an EBG substrate. IEEE Trans Antenn Propagat, 2009, 57: 926–935
24 Raad H R, Abbosh A I, Al-Rizzo H M, et al. Flexible and compact AMC based antenna for telemedicine applications. IEEE Trans Antenn Propagat, 2013, 61: 524–531
25 Yan S, Soh P J, Vandenbosch G A E. Low-profile dual-band textile antenna with artificial magnetic conductor plane. IEEE Trans Antenn Propagat, 2014, 62: 6487–6490
26 Lui K W, Murphy O H, Toumazou C. A wearable wideband circularly polarized textile antenna for effective power transmission on a wirelessly-powered sensor platform. IEEE Trans Antenn Propagat, 2013, 61: 3873–3876
27 Hertleer C, Rogier H, Vallozzi L, et al. A textile antenna for off-body communication integrated into protective clothing for firefighters. IEEE Trans Antenn Propagat, 2009, 57: 919–925
28 Locher I, Klemm M, Kirstein T, et al. Design and characterization of purely textile patch antennas. IEEE Trans Adv Packag, 2006, 29: 777–788
29 Yan Z, Pan T, Yao G, et al. Highly stretchable and shape-controllable three-dimensional antenna fabricated by "Cut-Transfer-Release" method. Sci Rep, 2017, 7: 42227
30 Zhang Y, Wang S, Li X, et al. Experimental and theoretical studies of serpentine microstructures bonded to prestrained elastomers for stretchable electronics. Adv Funct Mater, 2014, 24: 2028–2037
31 Fan J A, Yeo W H, Su Y, et al. Fractal design concepts for stretchable electronics. Nature Commun, 2014, 5: 3266
32 Jang K I, Li K, Chung H U, et al. Self-assembled three dimensional network designs for soft electronics. Nat Commun, 2017, 8: 15894